In utero exposure to dioxin causes neocortical dysgenesis through the actions of $p27^{Kip1}$

Takayuki Mitsuhashi[a], Junzo Yonemoto[b], Hideko Sone[b], Yasuhiro Kosuge[a,1], Kenjiro Kosaki[a], and Takao Takahashi[a,2]

[a]Department of Pediatrics, School of Medicine, Keio University, Shinjuku-ku, Tokyo 160-8582, Japan; and [b]Research Center for Environmental Risk, National Institute for Environmental Studies, Tsukuba-City, Ibaraki 305-8506, Japan

Edited by Pasko Rakic, Yale University, New Haven, CT, and approved July 13, 2010 (received for review March 8, 2010)

Dioxins have been reported to exert various adverse effects, including cell-cycle dysregulation in vitro and impairment of spatial learning and memory after in utero exposure in rodents. Furthermore, children born to mothers who are exposed to dioxin analogs polychlorinated dibenzofurans or polychlorinated biphenyls have developmental impairments in cognitive functions. Here, we show that in utero exposure to dioxins in mice alters differentiation patterns of neural progenitors and leads to decreased numbers of non-GABAergic neurons and thinner deep neocortical layers. This reduction in number of non-GABAergic neurons is assumed to be caused by accumulation of cyclin-dependent kinase inhibitor $p27^{Kip1}$ in nuclei of neural progenitors. Lending support to this presumption, mice lacking $p27^{Kip1}$ are not susceptible to in utero dioxin exposure. These results show that environmental pollutants may affect neocortical histogenesis through alterations of functions of specific gene(s)/protein(s) (in our case, dioxins), exerting adverse effects by altering functions of $p27^{Kip1}$.

environmental pollutants | cerebral cortex | development | neuronal progenitor cells | cell cycle

Dioxins are ubiquitous environmental pollutants that have been known to disturb hormonal homeostasis in mammals (1–3). In utero exposure to 2,3,7,8-tetrachlorodibenzo-*p*-dioxin (TCDD), one of the most potent dioxins, has been shown to cause impaired spatial learning and memory in rats (4). Furthermore, in humans, it is reported that children born to mothers who are exposed to dioxin analogs polychlorinated dibenzofurans (PCDFs) or polychlorinated biphenyls (PCBs) have developmental impairments in higher cognitive functions (2, 5). Additionally, a recent report describes the relationship between prenatal exposure level of polycyclic aromatic hydrocarbons and child intelligence at 5 y of age (6). However, the mechanisms by which dioxin exposure in utero affects the higher cortical functions after birth remain undetermined.

Non-GABAergic projection neurons, accounting for 80% of the neocortical neurons, are produced by proliferation/differentiation of neuronal progenitor cells (NPCs) constituting the pseudostratified ventricular epithelium [PVE; roughly coexistent with the ventricular zone (VZ)] along the lateral ventricular surface of the embryonic forebrain. The term PVE has been adopted, because it excludes postmitotic, premigratory neuroblasts of the subventricular zone (7, 8). In mice, the NPCs undergo 11 cell divisions during the period of neocortical histogenesis, with the length of the cell cycle (T_C) increasing by 2-fold from 8 to 18 h, mainly because of prolongation of the G1 phase of the cell cycle (T_{G1}) (8). During the same period, the proportion of daughter cells that become postmitotic during each cell cycle [quiescent (Q) fraction] increases (9). It is of critical importance that the layer position of the non-GABAergic projection neurons is strongly correlated with the cell cycle of origin (that is, the cell cycle at which a given non-GABAergic neuron becomes mitotically quiescent and starts radial migration to the neocortex) (10). Taken together, the regulated patterns of increase of the T_{G1} and Q fractions and strict correlation between the layer position and the cell cycle of origin both strongly suggest a link between cell-cycle regulation of the G1 phase and neuronal cell-class determination (layer destination of projection neurons) (10).

Progression of the cell cycle is precisely controlled by a set of proteins including cyclins, cyclin dependent kinases (CDKs), and CDK inhibitors (11). $p27^{Kip1}$, one of the CDK inhibitors, specifically inhibits the activity of cyclin E/CDK2 kinase and inhibits entry of the cells into the S phase (12, 13). Indeed, some of the critical events during the G1 phase of the cell cycle in NPCs are regulated by $p27^{Kip1}$: alterations in $p27^{Kip1}$ expression in the NPCs result in changes in the Q fraction, thereby altering the number of neurons to be produced and hence, the thickness of the neocortex. Specifically, overexpression of $p27^{Kip1}$ in NPCs in vivo increases the Q fraction (that is, promotes differentiation of the NPCs), with a resultant thinner neocortex (14, 15), whereas the lack of $p27^{Kip1}$ decreases the Q fraction, resulting in a thicker neocortex (16). It is worthy of note in this context that TCDD has been reported to induce $p27^{Kip1}$ and delay the G1 phase of the cell cycle in a hepatoma cell line, fetal thymocytes, and human neuronal cell line (17). Taken together, these observations suggest that in utero exposure to TCDD is likely to alter the proliferative behaviors of the NPCs by inducing $p27^{Kip1}$ protein expression, resulting in abnormalities of neocortical histogenesis.

Here, we report that in utero exposure to TCDD indeed modified the $p27^{Kip1}$ activities in NPCs to cause neocortical dysgenesis. These observations can be explained by a hypothetical mathematical model where both the increase in Q fraction and the neuronal class switch occur prematurely compared with that under physiological conditions.

Results

TCDD Exposure in Utero Reduced the Size of the Telencephalon and Thickness of the Neocortex as Assessed on Postnatal Day 21. The telencephalon, olfactory bulb, and cerebellum of TCDD-treated mice showed a normal appearance on postnatal day (P) 21 (Fig. 1*A*). However, the forebrains in these TCDD-treated animals were smaller, with the width and length being reduced by 4.78% (9.48 ± 0.063 mm vs. 9.93 ± 0.030 mm in the controls; $P < 0.001$, $n = 10$) and 2.29% (8.37 ± 0.048 vs. 8.57 ± 0.035 mm; $P = 0.004$, $n = 10$), respectively, compared with the values in the controls. The reductions in the width and length of the telencephalon indicate that TCDD exposure in utero caused roughly 7% reduction of the neocortical surface area. The thickness of the primary somatosensory cortex was reduced by 14.9% (750 ± 29.2 vs. 881.3 ± 13.2 μm; $P < 0.001$, $n = 6$) (Fig. 1*B*); the thickness of the deeper

Author contributions: T.M., J.Y., H.S., K.K., and T.T. designed research; T.M. and Y.K. performed research; T.M. and T.T. analyzed data; and T.M. and T.T. wrote the paper.

The authors declare no conflict of interest.

This article is a PNAS Direct Submission.

Freely available online through the PNAS open access option.

[1]Present address: Research Unit of Pharmacology, School of Pharmacy, Nihon University, Chiba 274-8555, Japan.

[2]To whom correspondence should be addressed. E-mail: ttakahashi@z3.keio.jp.

This article contains supporting information online at www.pnas.org/lookup/suppl/doi:10.1073/pnas.1002960107/-/DCSupplemental.

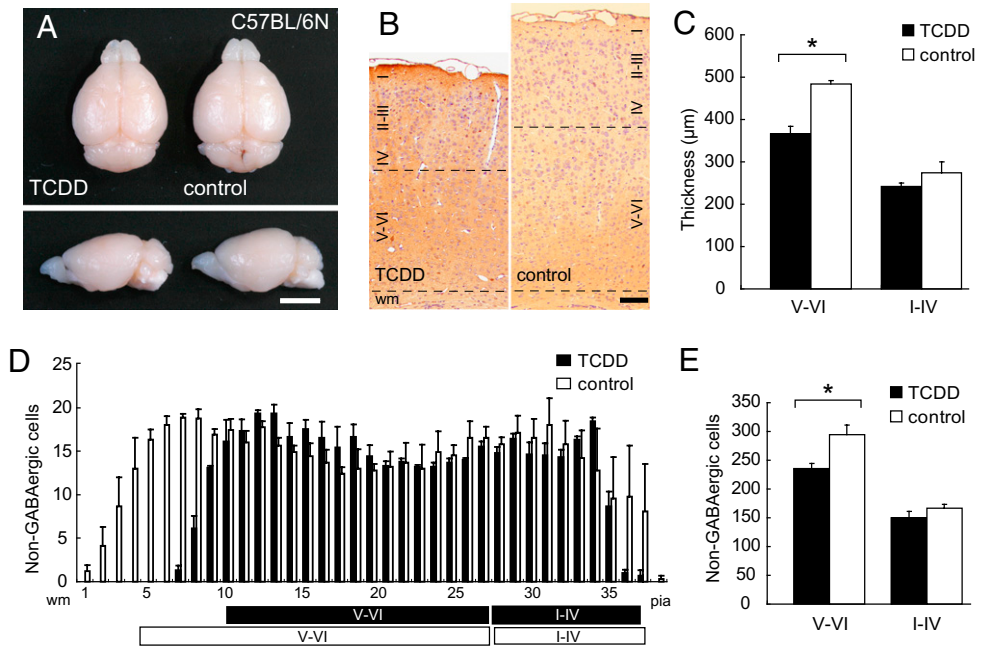

Fig. 1. Effects of in utero TCDD exposure observed on postnatal day 21. (*A*) Macroscopic dorsal and lateral overview of the whole brain from TCDD-treated and control C57BL/6N mice. (Scale bar, 5 mm.) (*B*) High-power view of the primary somatosensory neocortex of the TCDD-treated and control mice. Brown cells, GABA-positive interneurons; purple nuclei, either non-GABAergic projection neurons or glial cells; black dotted lines, boundaries between layers I-IV/V-VI and gray matter/white matter (wm). (Scale bar, 100 μm.) (*C*) Thickness of layers V-VI and I-IV in the TCDD-treated and control mice shown in *B*. (*D*) Numbers of non-GABAergic neurons counted in each bin (250 μm in width and 25 μm in height) lined serially from wm to the pial surface (pia) in the primary somatosensory neocortex shown in *B*. Black and white boxes under the abscissa indicate layers I-IV/V-VI in the neocortex of the TCDD-treated and control mice, respectively. (*E*) Total number of non-GABAergic neurons in layers V-VI and I-IV. *$P < 0.05$. Error bars in *C–E*, SEM.

cortical layers (layers V-VI) was reduced by 24.1% (366.7 ± 16.67 vs. 483.3 ± 8.33 μm; $P = 0.005$, $n = 6$), whereas no significant change in the thickness of the superficial layers (layers I-IV) was noted (241.7 ± 8.33 vs. 275.0 ± 25.0 μm; $P = 0.38$, $n = 6$) (Fig. 1*C*).

TCDD Exposure in Utero Reduced the Number of Non-GABAergic Neurons in the Deeper Cortical Layers as Assessed on Postnatal Day 21. We identified non-GABAergic projection neurons by the lack of positive immunohistochemical staining of the cells with anti-GABA antibody (Fig. 1 *B* and *D*). The number of non-GABAergic projection neurons in the primary somatosensory neocortex on P21 was significantly reduced in the deeper layers of the TCDD-treated animals by 20.0% compared with that in normal controls (Fig. 1*E*) (235.6 ± 9.24 vs. 294.3 ± 16.9 per 1,000 μm^2; $P = 0.037$, $n = 3$). However, there was no significant difference in the number of non-GABAergic neurons in the superficial layers of the cortex in the TCDD-treated animals compared with that in the controls (Fig. 1*E*) (149.8 ± 10.9 vs. 166.8 ± 6.14 per 1,000 μm^2; $P = 0.246$, $n = 3$). No alteration in the cell-packing density of the non-GABAergic projection neurons was observed in either the deeper or superficial layers in the TCDD-treated animals. Taken together, we concluded that the reduction in neocortical thickness of the TCDD-treated mice was caused by the reduction in the number of non-GABAergic projection neurons in the deeper cortical layers.

Total Cell Cycle Length of the NPCs Was Not Altered by TCDD Exposure in Utero. Next, we examined the TCDD-treated embryonic forebrains on E12, the time point at which the non-GABAergic neurons of the deeper layers (layers V–VI) are to be produced (10). Histologically, the dorsomedial cerebral wall, the future primary somatosensory neocortex, was normal in the TCDD-treated embryos (Fig. 2*A*). The S phase zone, where accumulation of the nuclei of the NPCs is observed during the S phase of the cell cycle, in the dorsomedial cerebral wall was located between 60 and 70 μm from the lateral ventricular border on E12 in the TCDD-treated mice, similar to the finding in the normal control mice (Fig. 2 *A* and *B*) ($n = 4$). At 4 h after exposure to bromodeoxyuridine (BrdU), BrdU-positive nuclei moved to the ventricular surface in both the TCDD-treated and control animals, indicating that the interkinetic nuclear migration in the embryonic forebrain operated normally in the TCDD-treated mice (Fig. 2*C*) ($n = 3$). After 6.5 h exposure to BrdU, virtually all of the nuclei in the VZ were BrdU-positive in both the TCDD-treated and control mice, indicating that the growth fractions in the VZ were nearly equal to 1.0 in both the TCDD-treated and control mice (Fig. 2*D*) ($n = 3$). The results of cumulative BrdU labeling (Fig. 2*E*) (18) revealed that the total cell-cycle length of the NPCs in the forebrain of the TCDD-treated animals was 10.7 h, not significantly different from that in the controls (Table 1).

TCDD Exposure in Utero Promoted Early Cell Cycle Exit of NPCs. We then identified the NPCs in the Q fraction and P fraction (the fraction of daughter cells that remain proliferative; $P = 1.0 - Q$) on E12 by using two S-phase tracers, iododeoxyuridine (IdU) and BrdU (Fig. 2*F*) (15, 19). In the dorsomedial cerebral wall of the TCDD-treated mice, the IdU-positive nuclei (blue nuclei) were located in the outer margin of the S-phase zone in both the P + Q and Q experiments (Fig. 2*F*). The distribution patterns of the P + Q and Q cells were not different between the TCDD-treated and control animals (Fig. 2*G*). An increase in the number of Q cells was observed in the TCDD-treated animals, with an estimated Q fraction of 0.17, which represented a 21.4% increase compared with the value in the controls (Table 2) ($n = 3$).

TCDD Exposure in Utero Increased the Nuclear Fraction of the p27^{Kip1} Protein in the NPCs. To elucidate the molecular mechanisms underlying the aforementioned changes, we first investigated the TCDD-induced changes in the mRNA expression levels of cell-cycle regulatory genes in the dorsomedial cerebral wall by dot blot hybridization (Fig. 3 *A* and *B*) ($n = 5$). We observed up-regulation

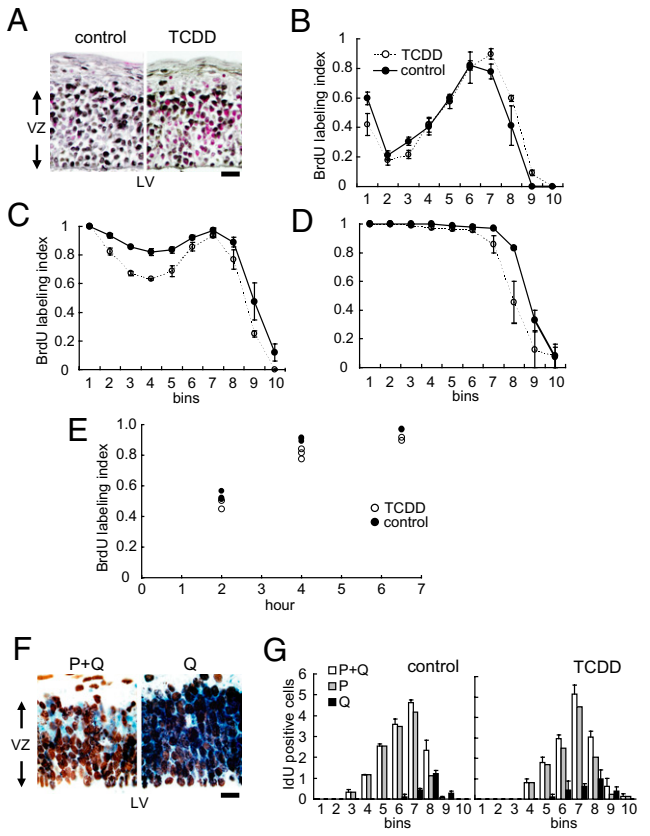

Fig. 2. Effects of in utero TCDD exposure on the cell-cycle kinetics of the NPCs. (*A*) High-power views of the dorsomedial cerebral wall of the E12 forebrains of the control and TCDD-treated mice. Black, BrdU-labeled nuclei; red, non–BrdU-labeled nuclei; VZ, ventricular zone; LV, lateral ventricle. (Scale bar, 10 μm.) (*B*) The 2-h BrdU-labeling index was evaluated in each bin (100 μm in width and 10 μm in height) lined serially from the lateral ventricle to the pial surface in the ventricular zone. The 4-h (*C*) and 6.5-h (*D*) BrdU-labeling indices are also shown. (*E*) Total labeling indices after cumulative BrdU exposure. (*F*) High-power views of the dorsomedial area of the E12 forebrains of mice exposed to TCDD. Blue nuclei, IdU-only positive; brown nuclei, double positive for IdU and BrdU. In the P + Q experiment (*Left*), blue nuclei correspond to the P + Q fraction cells. In the Q experiment (*Right*), blue cells correspond to only the Q fraction cells. (Scale bar, 10 μm.) (*G*) The number of Q fraction cells and P + Q fraction cells that were counted in each bin in control (*Left*) and TCDD-treated embryos (*Right*).

of the *p27*^{Kip1} and *p15*^{INK4b} mRNAs in the E12 forebrain in the TCDD-treated animals compared with the expressions in the controls (Fig. 3*B*): both *p27*^{Kip1} and *p15*^{INK4b} are CDK inhibitors that are known to promote exit from the cell cycle (11). We then analyzed the p27^{Kip1} and p15^{INK4b} protein levels by immunoblot analysis of lysates of the E12 dorsomedial cerebral walls. The p27^{Kip1} and p15^{INK4b} protein levels in the total tissue lysate were not significantly different between the TCDD-treated and control animals. However, when only the nuclear fractions from the dorsomedial cerebral wall were analyzed, the p27^{Kip1} protein level was about 2.5-fold higher in the TCDD-treated mice compared with the levels in the controls, the difference being significant (Fig. 3 *C* and *D*) ($n = 4$).

Table 1. Lengths of each phase of the cell cycle estimated by cumulative BrdU labeling index

	$T_C - T_S$	T_C	T_S	T_{G1}	T_{G2+M}
TCDD	7.0	10.7	3.7	5.0	2.0
Control	6.3	10.5	4.3	4.3	2.0

T_C, length of the total cell cycle; T_S, length of S phase, T_{G1}, length of G1 phase; T_{G2+M}, length of G2 + M phase.

Table 2. Q fraction analysis

	N_{P+Q}	N_Q	P fraction	Q fraction
TCDD	14.5	2.6	0.82	0.17
Control	14.7	2.1	0.86	0.14

N_{P+Q}, number of blue nuclei in the P + Q experiment; N_Q, number of blue nuclei in the Q experiment; Q fraction, N_Q/N_{P+Q}; P fraction, 1 − Q.

TCDD Exposure in Utero Did Not Reduce the Number of Non-GABAergic Neurons in the Deeper Cortical Layers of the p27^{Kip1} Knockout Mice. To further confirm the role of p27^{Kip1} in the events associated with TCDD exposure in utero, we repeated the in utero TCDD exposure experiments using p27^{Kip1} knockout mice (p27$^{-/-}$) (Fig. 4*A*) (20–22). We have previously reported that an increased thickness of the somatosensory neocortex on P21 in p27$^{-/-}$ mice compared with that in the wild-type animals is caused by the overproduction of non-GABAergic projection neurons destined for the superficial neocortical layers (16). Here, neither the layer thickness nor the number in non-GABAergic neurons of the primary somatosensory neocortex on P21 was significantly reduced in the TCDD-treated p27$^{-/-}$ compared with the findings in the controls (i.e., p27$^{-/-}$ mice exposed to corn oil; $n = 5$) (Fig. 4 *B–D*).

Discussion

Reduction in the Peak Population Size of NPCs by TCDD Exposure. The neocortical surface area, although influenced by multiple factors such as neuropil expansion and other growth-related parameters, is mostly determined during its ontogeny by the degree of tangential expansion of PVE (9). The size of the PVE, in turn, is virtually exclusively determined by the maximum population size of the NPCs, because dominant constituents of the PVE are the NPCs (9). Thus, the reduction of the neocortical surface area in the TCDD-treated mice (Fig. 1) strongly indicates a decrease in the maximum number of NPCs during neocortical histogenesis. The population size of the NPCs is governed solely by the pattern of ascent of the Q fraction during the early phase of neocortical histogenesis, and the maximum size is reached at the

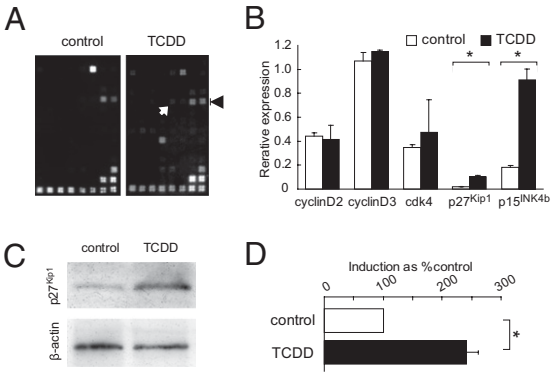

Fig. 3. Effects of in utero TCDD exposure on the expression profile of cell-cycle regulatory genes in the NPCs. (*A*) cDNA expression arrays hybridized with biotinylated probes generated from the embryonic forebrain of control and TCDD-treated mice. Black arrowhead and white arrow indicate signals from *p15*^{INK4b} and *p27*^{Kip1}, respectively. (*B*) mRNA expression after TCDD exposure. The β-actin signal equals 1.0. (*C*) Immunoblot analysis of nuclear p27^{Kip1} protein in the forebrains of the embryos of the control and TCDD-treated mice. β-actin levels were used to verify equal loading of the samples. (*D*) TCDD-induced increase of nuclear p27^{Kip1} protein. Bars, percentage signal intensity relative to the levels in the control embryos set at 100%. *$P < 0.05$. Error bars in *B* and *D*, SEM.

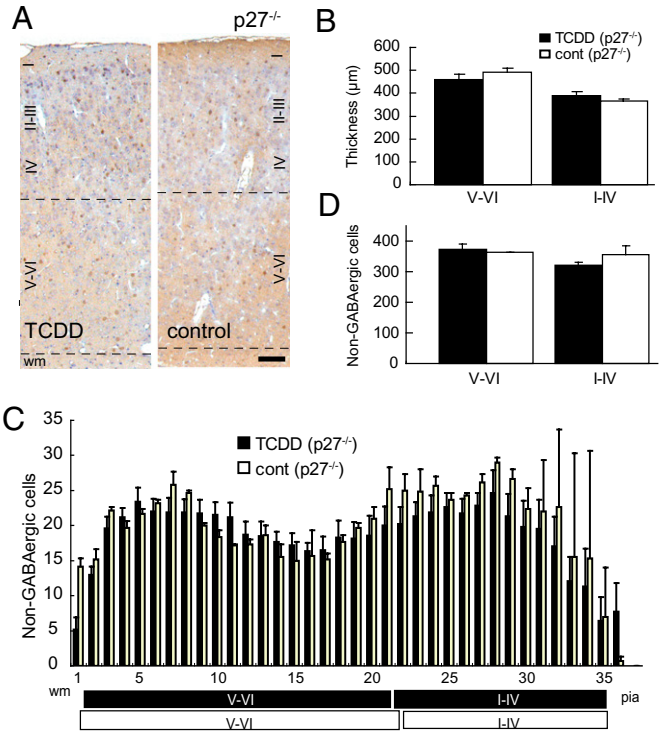

Fig. 4. Effects of in utero TCDD exposure in p27^{Kip1} knockout mice as assessed on P21. (*A*) High-power view of the primary somatosensory neocortex of p27^{Kip1} knockout mice (p27$^{-/-}$) exposed to TCDD and control mice. Brown cells, GABA-positive interneurons; purple nuclei, either non-GABAergic projection neurons or glial cells; black dotted lines, boundaries between layers I-IV/V-VI and gray matter/wm. (Scale bar, 100 μm.) (*B*) Thickness of layers V-VI and I-IV in the TCDD-treated and control mice shown in *A*. (*C*) Numbers of non-GABAergic neurons counted in each bin (250 μm in width and 25 μm in height) lined serially from the wm to the pia in the primary somatosensory neocortex shown in *A*. Black and white boxes under the abscissa indicate layers I-IV/V-VI in the neocortex of the TCDD-treated and control mice, respectively. (*D*) Total number of non-GABAergic neurons in layers V-VI and I-IV. Error bars in *B*–*D*, SEM.

point where the Q fraction reaches 0.5: the earlier the Q fraction reaches 0.5, the smaller the peak NPC population size (9, 23). Because no increase in apoptosis was noted in the PVE of the TCDD-treated mice, we conclude that TCDD exposure in utero reduced the peak population size of the NPCs by inducing a premature increase of the Q fraction. Because the degree of surface-area reduction is relatively small (7%), the premature increase in the Q fraction to 0.5 was likely to have occurred relatively late during the period, when the Q fraction was between 0 and 0.5. This assumption agrees with the previously reported p27^{Kip1} expression pattern among NPCs (that is, extremely low at the outset with the peak expression in the middle of neuronogenesis) (24).

Possible Mechanisms of Underproduction of Non-GABAergic Neurons in the Deeper Cortical Layers. It is of critical importance to note that only those projection neurons that are produced during the early phase of neuronogenesis when the Q fraction is less than 0.5 become destined for the deeper cortical layers (9, 10). It follows that the time point at which the Q fraction reaches 0.5 during neuronogenesis is the critical time window for the phenotypic switch from the deep- to superficial-layer neurons (25). Taken together, we conclude that the abnormal increase of the Q fraction during the early phase of neuronogenesis induced by TCDD exposure leads not only to a decrease of the peak population size of the NPCs but also to premature-cell phenotype switch and consequently, a decrease in the number of non-GABAergic projection neurons in the deeper cortical layers.

Of note, the progenitor population of the PVE is already committed to their lineage without pluripotency. In fact, our preliminary results indicated that GABAergic neurons and glial cells were also reduced in number, and such reduction was not observed in p27$^{-/-}$. It follows that p27^{Kip1} is likely to be responsible for determining the size of those neural populations as well. The proliferation/differentiation characteristics of progenitor populations of GABAergic neurons (NPCs of the ganglionic eminence) and glial cells surely deserve further investigation (26).

Mechanism of Nuclear Accumulation of p27^{Kip1} After TCDD Exposure. The premature increase of the Q fraction, as described in the foregoing paragraphs, is the underlying biological mechanism for the TCDD-induced abnormality of neocortical histogenesis. The increase of the Q fraction seems to be attributable to the nuclear accumulation of p27^{Kip1}: this hypothesis is lent strong support by the finding that mice lacking the p27^{Kip1} protein showed almost no alteration of the neocortical thickness after TCDD exposure (Fig. 4). Thus, p27^{Kip1} may be involved in the cascade of critical events anywhere downstream of the direct effect of TCDD. There has been no report to this date, to the best of our knowledge, on the effect of TCDD on the subcellular localization of the p27^{Kip1}. The nuclear fraction of p27^{Kip1} protein is determined by the balance of the protein transportation into and out of the nuclei. However, the expression levels of Jab-1, Akt, and Skp2 proteins, known to be involved in the nuclear transportation and degradation of the p27^{Kip1} protein, were not found to be altered in the NPCs of the TCDD-treated mice (27–31). Another intriguing observation is the stability of the total cell-cycle length observed, despite TCDD exposure (Table 1). The stabilizing mechanisms of the cell-cycle kinetics shown in *Drosophila melanogaster* (32) may also be involved in the homeostasis of the NPC cell cycle after in utero TCDD exposure.

This report quantitatively evaluates the effects of an environmental pollutant on neocortical histogenesis. In addition, this study is an example of an experimental model where the phenotypic severity of a particular adverse effect of a given environmental substance was found to be dependent on the genotype of the animals, which has profound implications from the viewpoint of toxicogenomics (33). Furthermore, our mathematical model of neocortical histogenesis has been shown to be a powerful tool to examine neocortical dysgenesis after relatively subtle alterations in the decision-making characteristics of the NPCs. We believe that this analytical method would be applicable to various environmental substances that may have adverse effects on human CNS development.

Materials and Methods

TCDD Administration. TCDD (Cambridge Isotope Laboratory) was dissolved in corn oil at a concentration of 2 μg mL^{-1}. A single dose of TCDD solution, or corn oil {0.01 mL [gram body weight (g bw)]$^{-1}$} as control, was administered orally to pregnant C57BL/6N and p27$^{-/-}$ mice on E7 using a disposable feeding needle. The total dose of TCDD administered was 20 μg (kg bw)$^{-1}$. This dose was adopted, because it was expected not to affect the mother in terms of child-rearing behavior. In fact, no adverse effect was observed during pregnancy and the postpartum period.

Measurement of the Dimensions of the Telencephalon. Brains from either TCDD- or corn oil-exposed mice on P21 were fixed in 4% phosphate-buffered formaldehyde containing 0.5% glutaraldehyde by transcardiac perfusion. The length and width of 10 telencephalons obtained from either TCDD- or corn oil-exposed P21 mice embryos were measured with micrometer calipers.

GABA Immunohistochemistry, Cumulative BrdU Labeling Analysis, and Q Fraction Analysis. GABA immunohistochemistry was performed as described previously using anti-GABA antibody (Chemicon International) (16). Cumulative BrdU labeling analysis (18) and Q fraction analysis (9, 15, 34) were performed as previously described. Detailed methods are described in *SI Materials and Methods*.

mRNA Expression Analysis and Immunoblot Analysis. Total RNA was isolated from E12 cerebral walls using the RNeasy Protect kit (Qiagen), and the mRNA was purified using the MicroPolyA Pure kit (Ambion) for generating biotinylated cDNA probes. The biotinylated probes were hybridized to cDNA expression arrays (GE array Q series Mouse Cell Cycle Gene Array; Superarray). Immunoblot analyses were conducted using anti-$p27^{Kip1}$, $p15^{INK4b}$, cyclin E, Skp2, β-actin (Santa Cruz Biotechnology), cyclin D1, CDK2, CDK4 (Sigma), AKT (Cell Signaling Technology), and Jab-1 (GeneTex) antibodies. Detailed methods are described in *SI Materials and Methods*.

ACKNOWLEDGMENTS. $p27^{Kip1}$ knockout mice were provided by Nippon Roche K.K. which were generated by Nakayama K, et al. (20). We acknowledge the assistance of Ms. H. Zaha and the discussions that we held with Drs. C. Tohyama and T. Goto during the preparation of this manuscript. This work was supported by Grant-in-Aid for Young Scientists (B) of the Ministry of Education, Culture, Sports, Science and Technology of Japan (17790723, 20790744, and 22791001 to T.M.) and Grant-in-Aid for Scientific Research (B) of Japan Society for the Promotion of Science (JSPS) (15390327, 18390302, and 20390299 to T.T.) and the 21st century Center of Excellence program of JSPS.

1. Barsotti DA, Abrahamson LJ, Allen JR (1979) Hormonal alterations in female rhesus monkeys fed a diet containing 2,3,7,8-tetrachlorodibenzo-p-dioxin. *Bull Environ Contam Toxicol* 21:463–469.
2. Birnbaum LS (1994) Endocrine effects of prenatal exposure to PCBs, dioxins, and other xenobiotics: Implications for policy and future research. *Environ Health Perspect* 102: 676–679.
3. Poland A, Knutson JC (1982) 2,3,7,8-tetrachlorodibenzo-p-dioxin and related halogenated aromatic hydrocarbons: Examination of the mechanism of toxicity. *Annu Rev Pharmacol Toxicol* 22:517–554.
4. Markowski VP, Cox C, Preston R, Weiss B (2002) Impaired cued delayed alternation behavior in adult rat offspring following exposure to 2,3,7,8-tetrachlorodibenzo-p-dioxin on gestation day 15. *Neurotoxicol Teratol* 24:209–218.
5. Chen YC, Guo YL, Hsu CC, Rogan WJ (1992) Cognitive development of Yu-Cheng ("oil disease") children prenatally exposed to heat-degraded PCBs. *JAMA* 268:3213–3218.
6. Perera FP, et al. (2009) Prenatal airborne polycyclic aromatic hydrocarbon exposure and child IQ at age 5 years. *Pediatrics* 124:e195–e202.
7. Sauer FC (1935) Mitosis in the neural tube. *J Comp Neurol* 62:377–405.
8. Takahashi T, Nowakowski RS, Caviness VS, Jr (1995) The cell cycle of the pseudostratified ventricular epithelium of the embryonic murine cerebral wall. *J Neurosci* 15:6046–6057.
9. Takahashi T, Nowakowski RS, Caviness VS, Jr (1996) The leaving or Q fraction of the murine cerebral proliferative epithelium: a general model of neocortical neuronogenesis. *J Neurosci* 16:6183–6196.
10. Takahashi T, Goto T, Miyama S, Nowakowski RS, Caviness VS, Jr (1999) Sequence of neuron origin and neocortical laminar fate: Relation to cell cycle of origin in the developing murine cerebral wall. *J Neurosci* 19:10357–10371.
11. Sherr CJ, Roberts JM (1999) CDK inhibitors: Positive and negative regulators of G1-phase progression. *Genes Dev* 13:1501–1512.
12. Toyoshima H, Hunter T (1994) p27, a novel inhibitor of G1 cyclin-Cdk protein kinase activity, is related to p21. *Cell* 78:67–74.
13. Polyak K, et al. (1994) Cloning of p27Kip1, a cyclin-dependent kinase inhibitor and a potential mediator of extracellular antimitogenic signals. *Cell* 78:59–66.
14. Mitsuhashi T, et al. (2001) Overexpression of p27Kip1 lengthens the G1 phase in a mouse model that targets inducible gene expression to central nervous system progenitor cells. *Proc Natl Acad Sci USA* 98:6435–6440.
15. Tarui T, et al. (2005) Overexpression of p27 Kip 1, probability of cell cycle exit, and laminar destination of neocortical neurons. *Cereb Cortex* 15:1343–1355.
16. Goto T, Mitsuhashi T, Takahashi T (2004) Altered patterns of neuron production in the p27 knockout mouse. *Dev Neurosci* 26:208–217.
17. Kolluri SK, Weiss C, Koff A, Göttlicher M (1999) p27(Kip1) induction and inhibition of proliferation by the intracellular Ah receptor in developing thymus and hepatoma cells. *Genes Dev* 13:1742–1753.
18. Takahashi T, Nowakowski RS, Caviness VS, Jr (1992) BUdR as an S-phase marker for quantitative studies of cytokinetic behaviour in the murine cerebral ventricular zone. *J Neurocytol* 21:185–197.
19. Nowakowski RS, Lewin SB, Miller MW (1989) Bromodeoxyuridine immunohistochemical determination of the lengths of the cell cycle and the DNA-synthetic phase for an anatomically defined population. *J Neurocytol* 18:311–318.
20. Nakayama K, et al. (1996) Mice lacking p27(Kip1) display increased body size, multiple organ hyperplasia, retinal dysplasia, and pituitary tumors. *Cell* 85:707–720.
21. Kiyokawa H, et al. (1996) Enhanced growth of mice lacking the cyclin-dependent kinase inhibitor function of p27(Kip1). *Cell* 85:721–732.
22. Fero ML, et al. (1996) A syndrome of multiorgan hyperplasia with features of gigantism, tumorigenesis, and female sterility in p27(Kip1)-deficient mice. *Cell* 85: 733–744.
23. Takahashi T, Nowakowski RS, Caviness VS, Jr (1997) The mathematics of neocortical neuronogenesis. *Dev Neurosci* 19:17–22.
24. Delalle I, Takahashi T, Nowakowski RS, Tsai LH, Caviness VS, Jr (1999) Cyclin E-p27 opposition and regulation of the G1 phase of the cell cycle in the murine neocortical PVE: A quantitative analysis of mRNA in situ hybridization. *Cereb Cortex* 9:824–832.
25. Caviness VS, Jr, et al. (2003) Cell output, cell cycle duration and neuronal specification: A model of integrated mechanisms of the neocortical proliferative process. *Cereb Cortex* 13:592–598.
26. Bhide PG (1996) Cell cycle kinetics in the embryonic mouse corpus striatum. *J Comp Neurol* 374:506–522.
27. Tomoda K, et al. (2002) The cytoplasmic shuttling and subsequent degradation of p27Kip1 mediated by Jab1/CSN5 and the COP9 signalosome complex. *J Biol Chem* 277: 2302–2310.
28. Kossatz U, et al. (2004) Skp2-dependent degradation of p27kip1 is essential for cell cycle progression. *Genes Dev* 18:2602–2607.
29. Carrano AC, Eytan E, Hershko A, Pagano M (1999) SKP2 is required for ubiquitin-mediated degradation of the CDK inhibitor p27. *Nat Cell Biol* 1:193–199.
30. Nakayama K, et al. (2000) Targeted disruption of Skp2 results in accumulation of cyclin E and p27(Kip1), polyploidy and centrosome overduplication. *EMBO J* 19:2069–2081.
31. Liang J, et al. (2002) PKB/Akt phosphorylates p27, impairs nuclear import of p27 and opposes p27-mediated G1 arrest. *Nat Med* 8:1153–1160.
32. Reis T, Edgar BA (2004) Negative regulation of dE2F1 by cyclin-dependent kinases controls cell cycle timing. *Cell* 117:253–264.
33. Shih DM, et al. (1998) Mice lacking serum paraoxonase are susceptible to organophosphate toxicity and atherosclerosis. *Nature* 394:284–287.
34. Hayes NL, Nowakowski RS (2000) Exploiting the dynamics of S-phase tracers in developing brain: Interkinetic nuclear migration for cells entering versus leaving the S-phase. *Dev Neurosci* 22:44–55.